Journal of Zhejiang University-SCIENCE A (Applied Physics & Engineering)
ISSN 1673-565X (Print); ISSN 1862-1775 (Online)
www.zju.edu.cn/jzus; www.springerlink.com
E-mail: jzus@zju.edu.cn

Multiphysics extension to physically based analyses of pipes with emphasis on frost actions

Zhen LIU[1], Xiong (Bill) YU[†‡1,2], Jun-liang TAO[1], Ye SUN[2]

([1]*Department of Civil Engineering, Case Western Reserve University, Cleveland, Ohio 44106, USA*)

([2]*Department of Electrical Engineering and Computer Science, Case Western Reserve University, Cleveland, Ohio 44106, USA*)

[†]E-mail: xxy21@case.edu

Received Sept. 7, 2012; Revision accepted Sept. 17, 2012; Crosschecked Sept. 7, 2012

Abstract: Pipes, especially buried pipes, in cold regions generally experience a rash of failures during cold weather snaps. However, the existing heuristic models are unable to explain the basic processes involving frost actions. This is because the frost action is not a direct load but one that causes variations in pipe-soil interactions resulting from the coupled thermo-hydro-mechanical process in soils. This paper developed and implemented a holistic multiphysics simulation model for freezing soils and extended it to the analysis of pipe-soil systems. The theoretical framework was implemented to analyze both static and dynamic responses of buried pipes subjected to frost actions. The multiphysics simulations reproduced phenomena commonly observed during frost actions, e.g., ice fringe advancement and an increase in the internal stress of pipes. The influences of important design factors, i.e., buried depth and overburden pressure, on pipe responses were simulated. A fatigue cracking criterion was utilized to predict the crack initialization under the joint effects of frost and dynamic traffic loads. The frost effects were found to have detrimental effects for accelerating fatigue crack initialization in pipes.

Key words: Underground pipe, Multiphysics, Frost action, Finite element method (FEM)
doi:10.1631/jzus.A12ISGT2 **Document code:** A **CLC number:** TU4

1 Introduction

Pipes have been used for the transportation of many chemically stable substances such as water (Walski, 1982), sewage (Fisher *et al.*, 2001), slurry (Doron *et al.*, 1987), oil (Nesic, 2007), natural gas (Konrad and Morgenstern, 1984) and other goods. They therefore do not only form an essential component of the urban and transportation infrastructure, but also serve as the lifeblood to the modern community (Rajani *et al.*, 1996; Moser, 2008). Unfortunately, their serviceability is jeopardized by intrinsic defects, environmental threats and inadequate installations (Rajani and Kleiner, 2001; Hu and Hubble, 2007). This situation turns out to be more serious when pipes are buried underground. This is because more factors, e.g., soil pressure, traffic loading, frost loads, and electro-chemical attacks can be involved as the pipes interact with ground soils and with a possible third party in or above the ground (Rajani and Kleiner, 2001; Makar, 2000).

The buried pipes are usually made of cast iron, ductile iron, polyvinyl chloride (PVC), polyethylene (PE), asbestos cement, or concrete. Taking water mains for example, cast iron pipes were extensively used to build water distribution systems from the 1900s until ductile iron pipes were introduced in the 1970s, followed by PVC water pipes which was introduced in Europe and North America during the 1970s, and more recently polyethylene pipes became widely accepted (Rajani *et al.*, 1996). It seems discouraging to find out that the physical mechanisms responsible for breakage vary from type to type leading to different failure modes such as circumferential break, longitudinal break, joint failure, holes

‡ Corresponding author

due to corrosion, and corporation cock failure. However, some trends have been found regardless of pipe types and failure modes. Among them, the detrimental effects of temperature, especially those of cold temperatures, have long been documented and investigated (Morris, 1967; Ciottoni, 1983).

This correlation between pipe failure risks and frost action has not only been frequently noticed in practice but has also been supported by experimental and theoretical analyses. Firstly, it is common knowledge among those involved in the management of water distribution systems that the onset of winter brings about an increase in maintenance activities (Papadopoulos and Welter, 2001). Similarly, as indicated in (Rajani *et al.*, 1996; Zhan and Rajani, 1997), the disruption of water services as a consequence of water main breaks is on the rise in most Canadian cities. The analysis of a typical annual pattern of break rate revealed that the peak in break frequency occurred during the period when ground temperatures were below normal. Similar studies (Needham and Howe, 1987; Lochbaum, 1993) on the performance of gas mains essentially reached the same conclusion. Morris (1967) and Ciottoni (1985) suggested that break frequency in winter was at least twice as high as that in summer, which was confirmed by field validation data (Rajani and Kleiner, 2001).

Both physically based methods (Rajani and Kleiner, 2001) and statistical methods (Kleiner and Rajani, 2001) have been employed for the analyses and designs of buried pipes. The strategy of physically based models is to evaluate or to predict the performance of buried pipes by investigating the physical behaviors consisting of various components, e.g., frictional resistance, thermal expansion, and residual structural resistance. The mechanical behaviors of most of these components were fairly well established and information is available through standards or textbooks (Young and Trott, 1984; Rajani and Kleiner, 2001; Moser, 2008). But it is also a consensus that an analytical procedure that satisfactorily explains why extreme cold temperatures lead to an increase in the number of water main breaks is still absent. In other words, the influence of frost temperature on the properties of pipes and surrounding soil and on the interactions between pipes and surrounding soil are unclear in existing theories.

Several reasons are responsible for the complexity of the frost effects. First of all, both pipes and surrounding soil suffer from a volume change in response to a temperature change but their thermal expansion coefficients can be very different. Furthermore, the phase change of pore water happens as the temperature drops below the freezing point. This will affect the heat transfer process since phase transition involves energy. There is no doubt that the formation of ice in pores can significantly alter soil properties such as elastic moduli. Moreover, there is a fluid transfer due to the temperature gradient (Philip and de Vries, 1957; Cary, 1965). The hydraulic process can be considerable and consequently changes not only the water and ice distributions but also the thermal and mechanical properties (e.g., volume change due to the phase transition of water and due to suction change resulting from the desaturation of water) of the pipe-soil system. Finally, the mechanical behavior is determined by the changes in the thermal and hydraulic fields as well as the constraints. Likewise, because of the existence of constraints (gravity, friction, etc.), the mechanical field can only respond partly to the other fields and thus in return affect the other fields. However, the aforementioned mechanisms are excluded in most existing studies. All the above phenomena can be coupled into a multiphysical process called thermo-hydro-mechanical process. The mechanisms beneath the multiphysics in soils have been extensively studied by researchers from soil science (Kay and Groenevelt, 1974; Sophocleous, 1979; Flerchinger and Pierson, 1991; Nassar and Horton, 1992; Scanlon and Milly, 1994; Noborio *et al.*, 1996a; 1996b; Nassar and Horton, 1997; Jansson and Karlberg, 2001) and civil engineering (Milly, 1982; Thomas *et al.*, 2009; Thomas and He, 1995; Sahimi, 1995; Noorishad *et al.*, 1992; Noorishad and Tsang, 1996. Stephansson *et al.*, 1997; Bai and Elsworth, 2000; Rutqvist *et al*., 2001; Wang *et al.*, 2009).

In this paper, a thermo-hydro-mechanical framework developed by the authors (Liu and Yu, 2011) is employed to explore the multiphysics of the pipe-soil system for buried pipes with an emphasis on frost actions. This model has been proven to allow for all of the aforementioned multiphysical phenomena and provides a computational capacity to tackle the high nonlinearity problem. In this paper, the soil model framework is extended to buried pipes. The main contributions of the study are given as follows.

1. It is the first time that a multiphysics (thermo-hydro-mechanical) model is employed for the analysis of buried pipes under freezing temperatures.

2. The phenomena that temperature drop cause advancing frost penetration in the surrounding soil and increase in the maximum stress are reproduced. The influences of two important parameters in the design of buried pipes in cold regions, i.e., buried depths and overburden pressures are analyzed;

3. The effect of random traffic loads in combination with the frost load on the fatigue failure of pipes is studied with fracture mechanics model.

2 Theoretical formulation

The multiphysics model presented by Liu and Yu (2011) included a thermal field, a hydraulic field, and a mechanical field. For each field, a governing partial differential equation was proposed in addition to a variety of auxiliary equations. Other coupled relationships such as the Clapeyron equation for describing the ice-water thermodynamic equilibrium were also incorporated. The model is briefly introduced in the following paragraphs. Detailed discussion can be found in the original paper (Liu and Yu, 2011).

2.1 Thermal field

To precisely formulate energy transport in porous materials, a modified Fourier's equation with both conduction and convection terms Eq. (1) was adopted as the governing equation for the thermal field.

$$C_a \frac{\partial T}{\partial t} = \nabla \cdot (\lambda \nabla T) - C_w \nabla (\boldsymbol{J} T), \tag{1}$$

where C_a is the overall apparent heat capacity, λ is the thermal conductivity of pipe or surrounding soil, T is the temperature, t is time, C_w is the heat capacity of unfrozen water and $\boldsymbol{J}$ is the water flux from the hydraulic field. Both C_a and λ are coupling variables. The moisture migration changes the soil composition and consequently C_a and λ, which in turn affects the heat transfer process. The convection term caused by water migration do only apply to soils.

The apparent volumetric heat capacity C_a in Eq. (1) takes into account the energy released/absorbed by the phase change of water. Instead of being treated as an energy sink or source on the right hand side of Fourier's equation, the enthalpy change due to the phase change can be incorporated into the heat capacity to reduce the nonlinearity (Anderson *et al.*, 1973).

$$C_a = C_{so}\theta_{so} + C_w\theta_w + C_i\theta_i + C_v(n - \theta_w - \theta_i) + L_f \frac{\mathrm{d}\theta_i}{\mathrm{d}t}, \tag{2}$$

where θ_{so}, θ_w, and θ_i denote the volumetric contents of soil mass, unfrozen water, and ice particles, respectively (The volume change of soil skeleton is neglected here). The same convention on subscripts applies to the other parameters, e.g., heat capacity. C_v is the heat capacity of air voids, and L_f is the latent heat.

The thermal conductivity λ in Eq. (1) can be approximated by empirical relationships such as Eq. (3) (Cass *et al.*, 1981; McInnes, 1981; Hansson *et al.*, 2004):

$$\lambda = C_1 + C_2(\theta_w + \theta_i F) - (C_1 - C_4) \cdot \exp\left\{-\left[C_3\left(\theta_w + \theta_i\right) + F\theta_i\right]^{C_5}\right\}, \tag{3}$$

$$F = 1 + F_1\theta_i^{F_2}, \tag{4}$$

where C_1, C_2, C_3, C_4, C_5, F_1, and F_2 are empirical curve fitting constants.

2.2 Hydraulic field

The mixed-type Richards' equation is generally used to describe the fluid movement in variably unsaturated porous media. The equation exhibits good performance in ensuring mass conservation (Celia and Binning, 1992). To extend the Richards' equation, a term related to ice formation is added to the left hand side of the Richards' equation to obtain

$$\frac{\partial \theta_w}{\partial t} + \frac{\rho_i}{\rho_w}\frac{\partial \theta_i}{\partial t} = \nabla \cdot (K_{Lh}\nabla h + K_{Lh}\boldsymbol{i} + K_{LT}\nabla T), \tag{5}$$

where ρ_w and ρ_i are the density of water and ice, respectively, K_{Lh} is the hydraulic conductivity, K_{LT} is the hydraulic conductivity due to thermal gradient, $\boldsymbol{i}$ is

the unit vector in the direction of gravity, and h is the matric potential head (or pressure head). The matric potential head is the equivalent water head (unit: m) of matric potential (unit: Pa). The two concepts are used interchangeably throughout this study.

$$S_e = \frac{\theta - \theta_r}{\theta_s - \theta_r} = (1+|\alpha h|^n)^{-m}, \quad (6)$$

where S_e is the effective saturation, h is the matric suction in the unit of water head, θ_s and θ_r are the saturated and residual water content, respectively, and α, m, and n are empirical parameters.

K_{Lh} and K_{LT} are hydraulic conductivities related to pore water head and temperature, respectively. One set of accepted relationships for these parameters are

$$K_{Lh} = K_s S_e [1-(1-S_e^{1/m})^m]^2, \quad (7)$$

$$K_{LT} = K_{Lh}\left(hG_{wT}\frac{1}{\gamma_0}\frac{d\gamma}{dT}\right), \quad (8)$$

where γ denotes the surface tension of soil water, which is temperature-dependent and can be approximated by γ=75.6−0.1425T−2.38×10$^{-4}T^2$; γ_0 is the value of γ at 25 °C, i.e., γ_0=71.89×10^{-3} kg·m^3.

As shown in Eq. (7), the hydraulic conductivity in partially saturated or partially frozen soil, K_{Lh}, is obtained by multiplying the saturated conductivity with a saturation-dependent 'relative conductivity' term. The thermally induced hydraulic conductivity in Eq. (8) was developed from the thermodynamics theory (Philip and de Vries, 1957). G_{wT} is a gain factor, which has a value around 7 for coarse-grained soils (Noborio *et al.*, 1996a; 1996b). The dependence of viscosity on temperature was neglected here to unify the equations for the intrinsic hydraulic conductivity and the hydraulic conductivity.

When phase changes are involved, the generalized Clapeyron Eq. (9) was used to describe the condition for the co-existence of water and ice. The local freezing point of pore fluid can be obtained from the generalized Clapeyron Eq. (9).

$$\frac{dh}{dT} = \frac{L_f}{gT}, \quad (9)$$

where h is the water head, L_f is the latent heat of water, and g is gravitational acceleration.

It is safe to assume that thermodynamic equilibriums are maintained at the ice-pore water interface at infinitesimal time intervals since the temperature change is negligible within such a short time interval. Hence, the Clapeyron equation can be used to determine the ice content via Eq. (10).

$$\frac{d\theta_i}{dT} = \frac{L_f}{gT}\frac{d\theta}{dT}. \quad (10)$$

2.3 Stress and strain fields

The governing equation for the stress and strain fields (mechanical field) is Navier's equation. It includes the equation of motion, strain-displacement correlation, and the constitutive relationship. The equation of motion (equation of equilibrium) is introduced in general tensor format as

$$\nabla\cdot(\boldsymbol{C}\nabla\boldsymbol{u}) + \boldsymbol{F} = \rho\ddot{\boldsymbol{u}} \ \left(\nabla\cdot(\boldsymbol{C}\nabla\boldsymbol{u}) + \boldsymbol{F} = 0\right), \quad (11)$$

where $\boldsymbol{u}$ is the displacement vector, $\boldsymbol{C}$ is the fourth-order tensor of material stiffness, and $\boldsymbol{F}$ is the body force vector.

The strain-displacement equation is

$$\boldsymbol{\varepsilon} = \frac{1}{2}[\nabla\boldsymbol{u} + (\nabla\boldsymbol{u})^T]. \quad (12)$$

The constitutive equation is

$$\boldsymbol{\sigma} = \boldsymbol{C} : \boldsymbol{\varepsilon}, \quad (13)$$

where $\boldsymbol{\sigma}$ is the Cauchy stress tensor, $\boldsymbol{\varepsilon}$ is the infinitesimal strain tensor, and the symbol ":" stands for double contraction.

In order to consider the influence of the thermal field and the hydraulic field on the stress field, the constitutive relationship for porous materials has to be formulated as

$$\boldsymbol{\sigma} = \boldsymbol{D}\boldsymbol{\varepsilon}_{el} + \boldsymbol{\sigma}_0, \quad (14)$$

where $\boldsymbol{D}$ is the stiffness matrix of soil skeleton, $\boldsymbol{\sigma}_0$ is the initial stress vector, and $\boldsymbol{\varepsilon}_{el}$ is the elastic strain which can be obtained from the following relationship,

$$\boldsymbol{\varepsilon} = \boldsymbol{\varepsilon}_{\mathrm{e1}} + \boldsymbol{\varepsilon}_{\mathrm{th}} + \boldsymbol{\varepsilon}_{\mathrm{tr}} + \boldsymbol{\varepsilon}_{\mathrm{hp}} + \boldsymbol{\varepsilon}_{0}, \tag{15}$$

where $\boldsymbol{\varepsilon}_{\mathrm{th}}$ is the strain caused by thermal expansion, $\left[\alpha(T - T_{\mathrm{ref}}), \alpha(T - T_{\mathrm{ref}}), 0\right]^{\mathrm{T}}$, T_{res} is the reference temperature set as the freezing temperature of water at normal conditions, 0 °C, $\boldsymbol{\varepsilon}_{\mathrm{tr}}$ is the strain caused by the phase change of water, which was approximated by $\left[0.09Q, 0.09Q, 0\right]^{\mathrm{T}}$ when a unit localization tensor in mixture theory is followed, in which Q is the degree of water phase transition, and 0.09 is the relative change of volume when water turns into ice; $\boldsymbol{\varepsilon}_0$ is the initial strain; $\boldsymbol{\varepsilon}_{\mathrm{hp}}$ is the strain resulting from the change of the matric potential, which is calculated by $[h / \boldsymbol{H}, h / \boldsymbol{H}, 0]^{\mathrm{T}}$. $\boldsymbol{H}$ is a parameter similar to the modulus corresponding to matric potential. The value of $\boldsymbol{H}$ can be obtained though experimental measurements. The use of $\boldsymbol{H}$ casts light on the independent role of matric potential in the constitutive relationship of unsaturated porous media as indicated in Biot's model for unsaturated fluid with air bubble and in Fredlund's method to address volume change of unsaturated soil (Biot, 1941; Fredlund and Rahardjo, 1993).

2.4 General boundary conditions

The general boundary condition, which includes the special cases such as the Dirichlet (first-type), Neumann (second-type) and Robin (third-type) boundary conditions, is formulated by

$$\boldsymbol{n} \cdot (c\nabla u + \varsigma u - \xi) + qu = \delta, \tag{16}$$

where $\boldsymbol{n}$ is the outward normal unit vector of a boundary, u is the dependent variable of individual field (temperature, matric potential, displacements, etc.), c is a conductivity term, ς is the conservative flux convection coefficient, ξ is the source in the computational domain, q is the boundary absorption coefficient, and δ is the boundary source.

3 Static analysis

The behaviors of porous materials under frost actions have been proven to be very complicated. Especially, there exist high nonlinearities when coupling effects are considered (Liu *et al.*, 2012). In addition, our pilot calculations found that solving 3D models demand excessive computational time. Due to the restriction of the computational resources, this study implemented model simulations under 2D geometries (plane strain conditions). A cross section of a pipe-soil system was chosen for both static and dynamic analyses. This section was assumed to be one representative of pipeline conditions. Non-homogeneities in the pipe and soil properties can be studied by varying the materials properties.

The static analysis mainly focus on the response of a buried pipe to subfreezing air temperature. The purpose was to examine if ground freezing can lead to increase of maximum tensile stress in the pipe. The effects of ground freezing were studied by comparing two different buried depths of pipe. In addition, the influence of overburden pressure was also studied since its influence on frozen ground has been extensively reported (Konrad and Morgenstern, 1982).

Three cases were studied in the static analysis: (1) pipe buried at a depth of 1 m (from the pipe center); (2) buried at a depth of 2.5 m; and (3) buried at a depth of 1 m and suffering from a constant overburden pressure of 0.1 MPa.

The configuration of a typical computational domain is illustrated by Fig. 1a. The mesh dimensions were chosen in a way that optimizes both model accuracy and computation efficiency. An initial air temperature of 6.7 °C was set. The temperature of the inner boundary for the pipe was assigned as 2 °C. This boundary condition was adopted in order to simulate a fluid of 2 °C running through the pipeline (operating temperature). Subsequently, the ground surface temperature was assumed to be maintained at −10 °C. The simulated duration under freezing was one month. The pipe was assumed to be a cast iron pipe with an outer diameter of 0.7 m and thickness of 0.03 m. The soil around the pipe was assumed to be an unsaturated soil (A6 soil according to AASHTO classification) with an initial volumetric water content of 0.33. The parameters used for the simulations are listed in Table 1.

An example of simulation results are presented in Fig. 1. The soil temperature dropped with the decrease of the air temperature. The frost penetration (frost front) went downwards to a depth ranging from 0.8 to 1 m in all of these three cases. The advancements of the frost penetration were similar in case 1

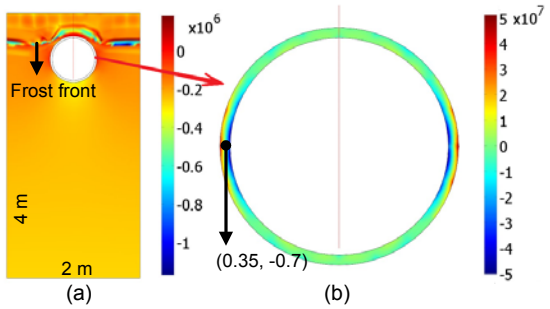

Fig. 1 Typical distribution of vertical stress in (a) soil and (b) pipe (unit: Pa)

Table 1 Parameters used for simulations of buried pipe

Parameter	Value	Parameter	Value
θ_0	0.33	λ_p (W/(m·K))	1.3
θ_r	0.031	C_{pp} (J/(m^3·K))	2×10^6
θ_{s0}	0.428	γ_p (kg/m^3)	7000
K_s (m/s)	5.806×10^{-6}	n	1.377
α (1/m)	1.202	m	0.274
H (m)	7653	μ	0.3

θ_0 is the initial water content, μ is the Poisson's ratio, H is the modulus related to pore pressure, C_{pp} is the volumetric heat capacity of pipe, and γ_p is the density of pipe

and case 3, although there was an observable difference between them. A general trend is the frost fronts curved slightly before they reached the crown of the pipe, due to the thermal boundary conditions inside the pipe. An ice arching developed as the frost front advanced beyond the depth of the pipe for cases 1 and 3. For case 2, the frost front was approximately level throughout the process. This is probably due to the fact that the influence of the pipe on the developments of frost front gets less significant at deeper burial depth. In all three cases, the internal stresses gradually increased both in the pipe and in the surrounding soil upon ground freezing. A typical distribution of vertical stresses is shown in Fig. 1. Fig. 1a clearly shows the arching effects that might be caused by ice front development.

The tensile stress plays an important role in pipe failure, especially for materials such as cast iron whose tensile strength is much lower than the compressive strength. The point associated with the maximum vertical tensile stresses is located near point (0.35, −0.7) or its symmetry point. Figs. 2–4 plots the time variations of the vertical tensile stresses in all of the three cases.

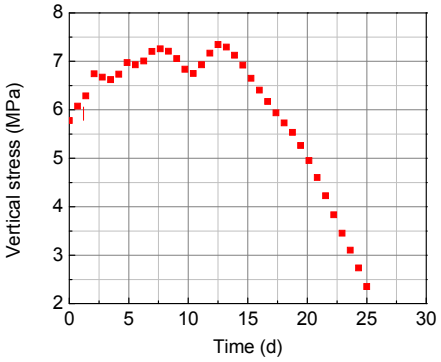

Fig. 2 Variation of vertical tensile stress for case 1

In case 1 (Fig. 2), the stress value increased with the development of freezing at the beginning. Note that the increase is dramatic. During that time, the pore water around the pipe migrated upwards to the regions above the pipe where substantial temperature gradients occurred. The increase in maximum vertical tensile stress slowed down as temperature at some locations dropped below the freezing point. The maximum vertical tensile stress continued increasing before it reached the peak at the 14th day. This is exactly the time when the front came into contact with the pipe crown. This simulated phenomenon reproduced that happened in field experiments (Smith, 1976). After that moment, the maximum tensile stress decreased rapidly to a value that was even smaller than its initial value. Meanwhile, we noticed that the shape of the frost front changed from a small curve to an arch around the upper part of the pipe (Fig. 1). Therefore, the increasing arching effect reduced the soil pressure and frost load on the top of the pipe. Moreover, the increasing soil modulus due to icing further added to the arching effects. The magnitude of simulated stress increase caused by frost actions is close to field measured data and results from other studies (Rajani *et al.*, 1996).

For case 2, where the pipe was buried in a depth larger than the maximum depth of frost penetration, the maximum vertical tensile stress was found be close to a constant (Fig. 3). There was slight oscillation of the stress with magnitude no more than 0.2 MPa. This might be a negligible error due to numerical errors, whose magnitude is much smaller in comparison with the absolute value of the maximum tensile stress. That is, the ground freezing effects on

the pipe in case 2 is rather limited. Detailed analysis found that there is not much change in the soil water content beneath the pipe. The depth of frost penetration is far from the buried depth of the pipe. This means that a deeper burial depth helps to alleviate climate effects under cold weather.

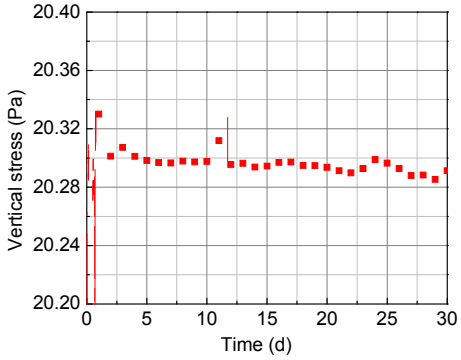

Fig. 3 Variation of vertical tensile stress for case 2

In case 3, overburden pressure was applied in addition to simulated frozen ground temperature. As can be seen in Fig. 4, the maximum tensile stress in the pipe varied in a similar way to that of case 1. The stress increases first and then decreases right after a peak, which is also on about the 14th day after freezing started. The same explanation is proposed for this pattern of variation in the maximum tensile stress. However, there are noticeable differences between the two cases. Firstly, the influence of subfreezing temperature on the pipe is amplified by the external load. Secondly, the decrease of stresses after passing the peak stress is not as rapid as that in case 1. Therefore, more attention is required for frost effects on pipes that are subjected to external loading.

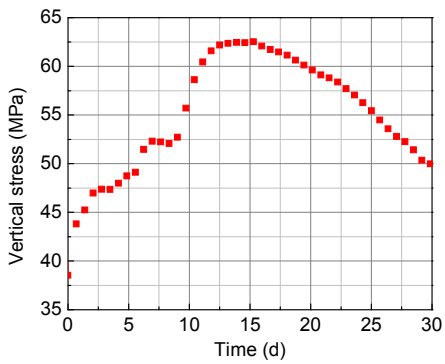

Fig. 4 Variation of vertical tensile stress for case 3

4 Dynamic analysis

The static simulations clearly demonstrated that the drop in the air temperature can cause significant increases in the internal stresses of buried pipes, a phenomenon that has been repeatedly documented. However, frost load is not the only factor accounting for pipe breaks during winter. Examination of historical records by the Cleveland Water Department, USA reveals a periodic resurging of pipe line fractures. This resembles a fatigue related failure pattern. Especially, pipes made from cast iron are believed to suffer mainly from fatigue failure (Margevicius and Haddad, 2002). To study the fatigue failure, the effects of dynamic loading (e.g., traffic load) on the fatigue life of pipes need to be studied in addition to the frost load.

The simulated geometry and boundary conditions were similar as that used for static study of pipes. A periodical sinusoidal loading was applied on the upper boundary (ground surface) to emulate traffic loading. For simplicity, the loading was assumed to be sinusoidal shape with a period of 1 h and an amplitude of 0.1 MPa. This long period was used to save computational time. Because the rate of frost front advancement is rather slow, the long dynamic duration was deemed feasible. In view of the results of the static analysis, a computational duration of one month was chosen to ensure there is enough time for freezing of the surrounding soil.

Both the stress obtained in the static and dynamic analyses was found to be far below the tensile strength of cast iron. This prompted us to pay primary attention to the high-cycle fatigue for which more than 10^4 cycles are required for failure. The fatigue crack growth rate equation from Forman *et al*. (1967), which is a modified version of Paris' equation, was employed,

$$\frac{\mathrm{d}a}{\mathrm{d}N}=\frac{C\Delta K^n}{(1-R)K_\mathrm{c}-\Delta K}, \tag{17}$$

where C and n are the exponent and coefficient in Forman *et al*. (1967)'s equation, and equal to 4.006×10^{-9} and 3.18255, respectively, R is the stress ratio, and ΔK is the intensity factor range.

Dynamic load, such as real traffic load, mostly

varies in magnitude. Even for repeated dynamic loads of the same magnitude, the response (maximum and minimum stresses) can still be different because frost is continuously developing due to variation of ground conditions. Root mean squared approach, which is a fatigue life prediction model for random loading conditions, was therefore utilized. This model provides a simple, reliable, and efficient method to predict fatigue crack growth in a structural component under random loading conditions (Kim *et al*., 2006). The mathematic formulation for this method is given in Eqs. (18) and (19). These formulas were implemented in the computational simulations.

$$\Delta K=\left\{\left[\frac{1}{M}\sum_{i-1}^{M}(\sigma_{\max})^2\right]^{1/2}-\left[\frac{1}{M}\sum_{i-1}^{M}(\sigma_{\min})^2\right]^{1/2}\right\}\cdot\sqrt{\frac{\pi a}{Q}}M_{\mathrm{e}}, \tag{18}$$

$$R=\left[\frac{1}{M}\sum_{i-1}^{M}(\sigma_{\min})^2\right]^{1/2}\Big/\left[\frac{1}{M}\sum_{i-1}^{M}(\sigma_{\max})^2\right]^{1/2}, \tag{19}$$

where $\sigma_{\min}$ and $\sigma_{\max}$ are the minimum and maximum stresses derived from random stress history, respectively, M is the total number of circles, and M_{e} can be obtained through shape properties of crack such as crack depth a and length c (Kim *et al*., 2006).

Model simulation results show that the point (0.35, −0.7) is one of the critical points on the pipe. The variation of the maximum tensile stress at this point was therefore employed for the dynamics analysis. As shown in Fig. 5, the maximum tensile stress increases as temperature decreases. This condition is similar to the seasonal frost that happens after the onset of the winter. There is a peak in the maximum tensile stress between the 14th and 17th day after freezing begins. After that, the maximum tensile stress decreased slightly and then increased again. This trend is distinct from the trend of maximum vertical stress observed in static analysis. The increasing arching effect is assumed to be the main causes in observed dynamic responses. The response of the unfrozen pipe-soil system subjected to the same dynamic load has also been simulated. The pattern of variation in the maximum tensile stress does not change with time in this case (Fig. 5).

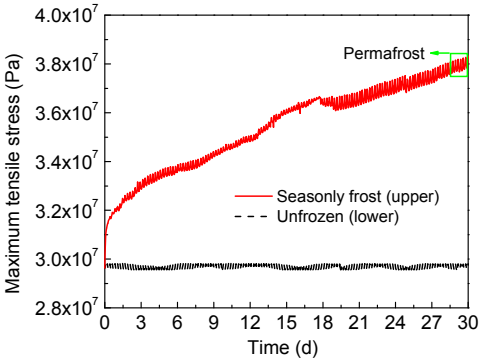

Fig. 5 Variation of maximum tensile stress in pipe

For three different conditions, i.e., unfrozen condition (no ground ice formation), seasonal frost (where the ice front advances less than the bury depth of pipe), and permafrost (where the ice front advances more than the bury depth of pipe), the influence of frost action on pipe fatigue was simulated by assuming that the fatigue life of the pipe is controlled by the variations in the maximum tensile stress. Fig. 6 simulated the crack development in the pipe under these conditions. It takes different lengths for the depth of crack to develop from an initial crack depth of 1.2 mm to the thickness of the pipe of 30 mm in three conditions. Pipe failures were assumed to happen as the depth of crack reaches the thickness of the pipe. The number of stress cycles, or fatigue life, was found to decrease by 50% as the pipe transferred from the unfrozen condition to the seasonal frost. The condition turned out to be even worse in the permafrost condition. The calculation thus directly illustrates the reduction in fatigue life as frost temperature happens. The combined effects of frost action and traffic loading further accelerate pipe fatigue fracture in cold regions.

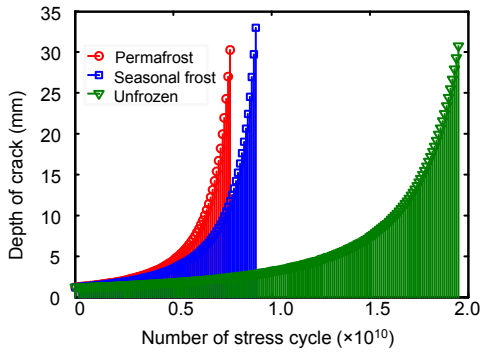

Fig. 6 Fatigue life prediction under different climate conditions

5 Conclusions

This paper conducted multiphysics simulations to study the effects of ground freezing on pipe performance. A multiphysics model was formulated to couple the thermo-hydro-mechanical process in frozen ground. The soil-structure interactions were considered in the simulation model. The model was implemented in 2D finite element method simulations. Both static and dynamic cases were studied. The results indicated that the ground freezing caused an appreciable increase in the stresses in pipes. The pipe burial depth and the overburden pressure were found to have important effects on the induced stresses in pipes. The dynamics of crack development in the pipe in response to the combination of traffic and frost load was investigated using a fracture dynamics model. The results indicated that the combined effects of ground freezing and dynamic loading can significantly shorten the service life of pipes. Besides reproducing the engineering observations, the current study demonstrates the capacity of the holistic multiphysics simulation for studying the frost effects on underground pipes. This study succeeded in providing a multiphysics extension to the physically based methods for the analysis and design of buried pipes, especially those in cold regions.

Acknowledgements

The authors gratefully acknowledge the Ohio Department of Transportation and Cleveland Water Division, USA.

References

Anderson, M., Tice, A.R., McKim, H.L., 1973. The Unfrozen Water and the Apparent Specific Heat Capacity of I Frozen Soils. Permafrost, North American Contribution to the 2nd International Conference, National Academy of Sciences, Washington, DC.

Bai, M., Elsworth, D., 2000. Coupled Processes in Subsurface Deformation, Flow and Transport. ASCE Press, Reston, VA.

Biot, M.A., 1941. General theory of three-dimensional consolidation. *Journal of Applied Physics*, **12**(2):155-164. [doi:10.1063/1.1712886]

Cary, J.W., 1965. Water flux in moist soil: thermal versus suction gradients. *Soil Science*, **100**(3):168-175. [doi:10.1097/00010694-196509000-00004]

Cass, A.G., Campbell, G.S., Jones, T.L., 1981. Hydraulic and Thermal Properties of Soil Samples from the Buried Waster Test Facility. PNL-4015. Pacific Northwest Laboratory, Richland, WA.

Celia, M.A., Binning, P., 1992. A mass conservative numerical solution for two-phase flow in porous media with application to unsaturated flow. *Water Resources Research*, **28**(10):2819-2828. [doi:10.1029/92WR01488]

Ciottoni, A.S., 1983. Computerized Data Management in Determining Causes of Water Main Breaks: the Philadelphia Case Study. Proceedings of the International Symposium on Urban Hydrology, Hydraulics and Sediment Control, University of Kentucky, Lexington, KY.

Ciottoni, A.S., 1985. Updating the New York City Water System. Proceedings of the Specialty Conference on Infrastructure for Urban Growth, San Diego, USA, p.69-77.

Doron, P., Granica, D., Barnea, D., 1987. Slurry flow in horizontal pipes: experimental and modeling. *International Journal of Multiphase Flow*, **13**(4):535-547. [doi:10.1016/0301-9322(87)90020-6]

Fisher, K., Bullen, F., Beal, D., 2001. The durability of cellulose fibre reinforced concrete pipes in sewage applications. *Cement and Concrete Research*, **31**(4):543-553. [doi:10.1016/S0008-8846(00)00451-8]

Flerchinger, G.N., Pierson, F.B., 1991. Modeling plant canopy effects on variability of soil temperature and water. *Agricultural and Forest Meteorology*, **56**(3-4):227-246. [doi:10.1016/0168-1923(91)90093-6]

Forman, R.G., Kearney, V.E., Engle, R.M., 1967. Numerical analysis of crack propagation in cyclic-loaded structures. *Journal of Basic Engineering*, **89**:459-464.

Fredlund, D.G., Rahardjo, H., 1993. Soil Mechanics for Unsaturated Soils. Wiley, New York. [doi:10.1002/9780470172759]

Hansson, K., Simunek, J., Mizoguchi, M., Lundin, L.C., van Genuchten, M.T., 2004. Water flow and heat transport in frozen soil: numerical solution and freeze-thaw applications. *Vadose Zone Journal*, **3**(2):693-704. [doi:10.2136/vzj2004.0693]

Hu, Y., Hubble, D.W., 2007. Factors contributing to the failure of asbestos cement water mains. *Canadian Journal of Civil Engineering*, **34**(5):608-621. [doi:10.1139/l06-162]

Jansson, P.E., Karlberg, L., 2001. Coupled Heat and Mass Transfer Model for Soil-Plant-Atmosphere Systems. Royal Institute of Technology, Department of Civil and Environmental Engineering, Stockholm.

Kay, B.D., Groenevelt, P.H., 1974. On the interaction of water and heat transport in frozen and unfrozen soils: I. basic theory: the vapor phase. *Soil Science Society of America Journal*, **38**(3):395-400. [doi:10.2136/sssaj1974.03615995003800030011x]

Kim, S.T., Tadjiev, D., Yang, H.T., 2006. Fatigue life prediction under random loading conditions in 7475-T7351 aluminum alloy using the RMS model. *International Journal of Damage Mechanics*, **15**(1):89-102.

[doi:10.1177/1056789506058605]

Kleiner, Y., Rajani, B.B., 2001. Comprehensive review of structural deterioration of water mains: statistical models. *Urban Water*, **3**(3):131-150. [doi:10.1016/S1462-0758(01)00033-4]

Konrad, J.M., Morgenstern, N.R., 1982. Effects of applied pressure of freezing soils. *Canadian Geotechnical Journal*, **19**(4):494-505. [doi:10.1139/t82-053]

Konrad, J.M., Morgenstern, N.R., 1984. Frost heave prediction of chilled pipelines buried in unfrozen soils. *Canadian Geotechnical Journal*, **21**(1):100-115. [doi:10.1139/t84-008]

Liu, Z., Yu, X., 2011. Coupled thermo-hydro-mechanical model for porous materials under frost action: theory and implementation. *Acta Geotechnica*, **6**(2):51-65. [doi:10.1007/s11440-011-0135-6]

Liu, Z., Sun, Y., Yu, X., 2012. Theoretical basis for modeling porous geomaterials under frost action: a review. *Soil Science Society of American Journal*, **76**(2):313-330. [doi:10.2136/sssaj2010.0370]

Lochbaum, B.S., 1993. PSE&G develop models to predict main breaks. *Pipeline Gas J.*, **220**:20-27.

Makar, J.M., 2000. A preliminary analysis of failures in grey cast iron water pipes. *Engineering Failure Analysis*, **7**(1):43-53. [doi:10.1016/S1350-6307(99)00005-9]

Margevicius, A., Haddad, P., 2002. Catastrophic Failures of Cleveland's Large Diameter Water Mains. Proceedings of Pipeline Division Specialty Conference, p.1-48. [doi:10.1061/40641(2002)25]

Milly, P.C.D., 1982. Moisture and heat transport in hysteretic, inhomogeneous porous media: a matric head-based formulation and a numerical model. *Water Resources Research*, **18**(3):489-498. [doi:10.1029/WR018i003p00489]

McInnes, K.J., 1981. Thermal Conductivities of Soils from Dryland Wheat Regions of Eastern Washington. MS Thesis, Washington State University, Pullman.

Morris, B.S., 1967. Principal causes and remedies of water main breaks. *Journal of American Water Works Association*, **54**:782-798.

Moser, A.P., 2008. Buried Pipe Design. McGraw-Hill Companies, Inc., New York.

Nassar, I.N., Horton, R., 1992. Simultaneous transfer of heat, water, and solute in porous media: I. theoretical development. *Soil Science Society of America Journal*, **56**(5):1350-1356. [doi:10.2136/sssaj1992.03615995005600050004x]

Nassar, I.N., Horton, R., 1997. Heat, water, and solute transfer in unsaturated porous media: I-theory development and transport coefficient evaluation. *Transport in Porous Media*, **27**(1):17-38. [doi:10.1023/A:1006583918576]

Needham, D., Howe, M., 1987. Why gas mains fail. part 1. *Pipe Line Industry*, **55**:47-50.

Nesic, S., 2007. Key issues related to modelling of internal corrosion of oil and gas pipelines: a review. *Corrosion Science*, **49**(12):4308-4338. [doi:10.1016/j.corsci.2007.06.006]

Noborio, K., McInnes, K.J., Heilman, J.L., 1996a. Two-dimensional model for water, heat and solute transport in furrow-irrigated soil: I. theory. *Soil Science Society of America Journal*, **60**(4):1001-1009. [doi:10.2136/sssaj1996.03615995006000040007x]

Noborio, K., McInnes, K.J., Heilman, J.L., 1996b. Two-dimensional model for water, heat, and solute transport in furrow-irrigated soil: II. field evaluation. *Soil Science Society of America Journal*, **60**(4):1010-1021. [doi:10.2136/sssaj1996.03615995006000040008x]

Noorishad, J., Tsang, C.F., 1996. Coupled Thermo-Hydro-Elasticity Phenomena in Variably Saturated Fractured Porous Rocks-Formulation and Numerical Solution. *In*: Coupled Thermo-Hydro-Mechanical Processes of Fractured Media, Elsevier, Rotterdam.

Noorishad, J., Tsang, C.F., Witherspoon, P.A., 1992. Theoretical and field studies of coupled hydromechanical behaviour of fractured rocks-1: development and verification of a numerical simulator. *International Journal of Rock Mechanics and Mining Science & Geomechanical Abstracts*, **29**(4):401-409.

Papadopoulos, G., Welter, G.J., 2001. Predicting Water Main Breaks in Winter. *In*: New Horizons in Drinking Water Annual Conference, Washington, DC.

Philip, J.R., de Vries, D.A., 1957. Moisture movement in porous materials under temperature gradients. *Transactions, American Geophysics Union*, **38**(2):222-232.

Rajani, B., Kleiner, Y., 2001. Comprehensive review of structural deterioration of water mains: physically based models. *Urban Water*, **3**(3):151-164. [doi:10.1016/S1462-0758(01)00032-2]

Rajani, B., Zhan, C., Kuraoka, S., 1996. Pipe-soil interaction analysis of jointed water mains. *Canadian Geotechnical Journal*, **33**(3):393-404. [doi:10.1139/t96-061]

Rutqvist, J., Börgesson, L., Chijimatsu, M., Kobayashi, A., Jing, L., Nguyen, T.S., Noorishada, J., Tsang, C.F., 2001. Thermo-hydro-mechanics of partially saturated geological media: governing equations and formulation of four finite element models. *International Journal of Rock Mechanics and Mining Science & Geomechanical Abstracts*, **38**(1):105-127.

Sahimi, M., 1995. Flow and Transport in Porous Media and Fractured Rock: from Classical Methods to Modern Approaches. VCH, Weinheim, Germany.

Scanlon, B.R., Milly, P.C.D., 1994. Water and heat fluxes in desert soils 2: numerical simulations. *Water Resources Research*, **30**(3):721-733. [doi:10.1029/93WR03252]

Smith, W.H., 1976. Frost loadings on underground pipe. *Journal of American Water Works Association*, **68**(12):673-674.

Sophocleous, M., 1979. Analysis of water and heat in unsaturated-saturated porous media. *Water Resources Research*, **15**(5):1195-1206. [doi:10.1029/WR015i005p01195]

Stephansson, O., Jing, L., Tsang, C.F., 1997. Coupled Thermo-Hydro-Mechanical Processes of Fractured Media. Elsevier, Rotterdam.

Thomas, H.R., He, Y., 1995. Analysis of coupled heat, moisture and air transfer in a deformable unsaturated soil. *Geotechnique*, **45**(4):677-689. [doi:10.1680/geot.1995.45.4.677]

Thomas, H.R., Cleall, P., Li, Y.C., Harris, C., Kern-Luetschg, M., 2009. Modelling of cryogenic processes in permafrost and seasonally frozen soils. *Geotechnique*, **59**(3):173-184. [doi:10.1680/geot.2009.59.3.173]

Walski, T.M., 1982. Economic analysis of water main breaks. *Journal of American Water Works Association*, **74**(3): 140-147.

Wang, W., Kosakowski, G., Kolditz, O., 2009. A parallel finite element scheme for thermo-hydro-mechanical (THM) coupled problems in porous media. *Computers & Geosciences*, **35**(8):1631-1641. [doi:10.1016/j.cageo.2008.07.007]

Young, O.C., Trott, J.J., 1984. Buried Rigid Pipes. Elsevier, London.

Zhan, C., Rajani, B., 1997. Estimation of frost load in a trench: theory and experiment. *Canadian Geotechnical Journal*, **34**(4):568-579. [doi:10.1139/cgj-34-4-568]